Dissociation from DNA of Type III Restriction–Modification enzymes during helicase-dependent motion and following endonuclease activity

Júlia Tóth, Kara van Aelst, Hannah Salmons and Mark D. Szczelkun*

DNA–Protein Interactions Unit, School of Biochemistry, Medical Sciences Building, University of Bristol, Bristol, BS8 1TD, UK

ABSTRACT

DNA cleavage by the Type III Restriction–Modification (RM) enzymes requires the binding of a pair of RM enzymes at two distant, inversely orientated recognition sequences followed by helicase-catalysed ATP hydrolysis and long-range communication. Here we addressed the dissociation from DNA of these enzymes at two stages: during long-range communication and following DNA cleavage. First, we demonstrated that a communicating species can be trapped in a DNA domain without a recognition site, with a non-specific DNA association lifetime of ~200 s. If free DNA ends were present the lifetime became too short to measure, confirming that ends accelerate dissociation. Secondly, we observed that Type III RM enzymes can dissociate upon DNA cleavage and go on to cleave further DNA molecules (they can 'turnover', albeit inefficiently). The relationship between the observed cleavage rate and enzyme concentration indicated independent binding of each site and a requirement for simultaneous interaction of at least two enzymes per DNA to achieve cleavage. In light of various mechanisms for helicase-driven motion on DNA, we suggest these results are most consistent with a thermally driven random 1D search model (i.e. 'DNA sliding').

INTRODUCTION

The bacterial/archaeal Type III Restriction–Modification (RM) enzymes specifically bind short, asymmetric DNA recognition sequences (5′-CAGCAG-3′ for EcoP15I or 5′-AGACC-3′ for EcoPI) and, following ATP hydrolysis by superfamily 2 (SF2) helicase domains in the Res subunits, produce a dsDNA break 25–27 bp downstream (3′) of the site (1–3). For efficient cleavage to occur in vitro (i.e. at relatively low enzyme concentrations and under stringent buffer conditions), two recognition sites must be present on the same DNA molecule in an inverted repeat orientation, either head-to-head (HtH) or tail-to-tail (TtT) (Figure 1) (4–6). These sites can be many thousands of base pairs apart (4), but can also be immediately adjacent to one another, or even overlapping (7). An ATP-driven, long-range communication event must occur to check for the presence of the two sites in the correct orientation on the same DNA molecule (8). Following this interaction, DNA cleavage occurs at only one of the two sites, although 10-fold slower cleavage of the remaining site ('secondary cleavage') can occur under relaxed reaction conditions (9,10). There is no evidence that Type III RM enzymes are DNA unwinding enzymes, the classically defined enzymatic role of a 'helicase' (11). However, there are many examples of helicases that couple ATP hydrolysis to other functions such as translocation of intact dsDNA, e.g. Type I RM enzymes (12) and chromatin remodelling enzymes (13). A key question is: how do the SF2 helicase domains of the Type III RM enzymes couple ATP hydrolysis to motion over thousands of base pairs?

A number of models have been proposed to account for the long-range communication by Type III RM enzymes (8,14,15). The loop translocation model (5,16–18), proposes that the helicase domains are involved in ATP-dependent stepwise unidirectional translocation of intact dsDNA while the methyltransferase remains bound to the site. A modified translocation model without DNA looping has also been proposed (19). Evidence for looping during motion has been obtained using atomic force microscopy (AFM) (16–18), but data obtained using a magnetic tweezers apparatus did not find evidence for obligatory long-lived DNA looping on pathway to cleavage (20). A key observation is that the
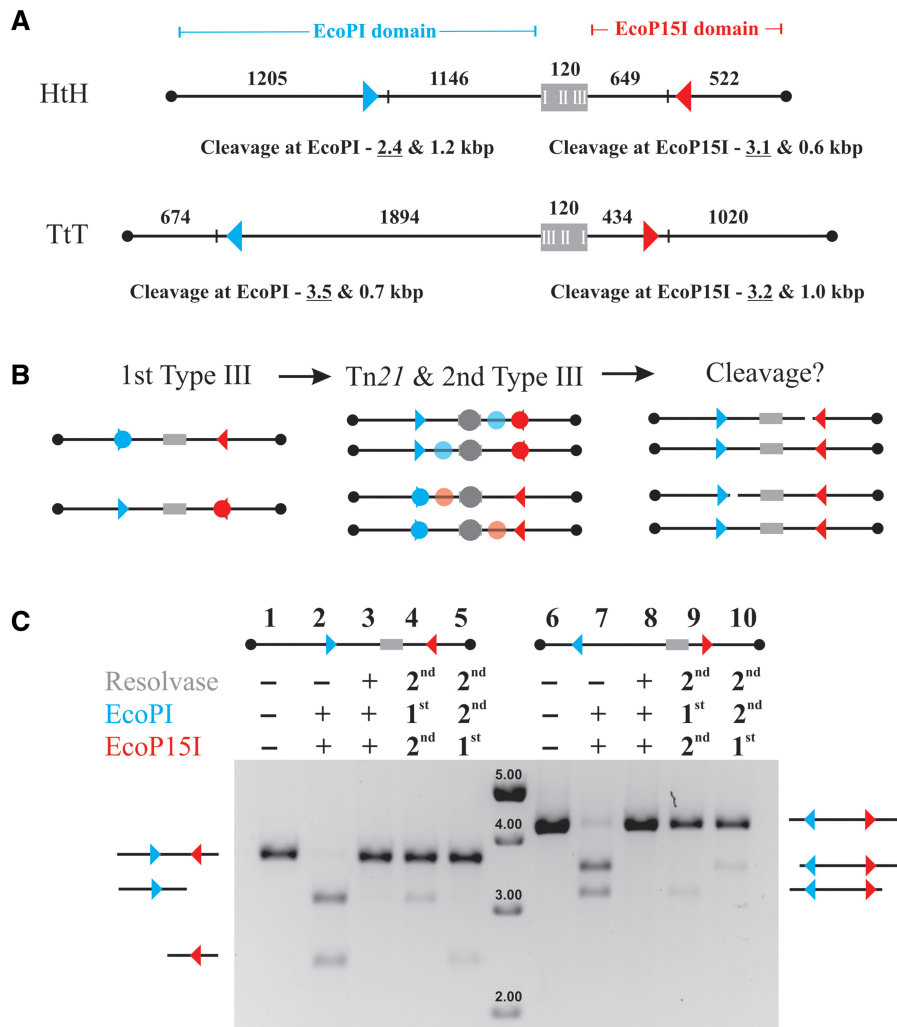
Figure 1. Design of the roadblock assay and evidence for bidirectional motion on DNA by Type III restriction enzymes. DNA is shown as a black line, Type III sites as directional arrowheads (blue, EcoPI; red, EcoP15I) with the cleavage sites as tick marks, the Tn*21 res* site as a grey box and biotin–streptavidin roadblocks as black circles. Distances are indicated in base pairs. (**A**) HtH and TtT mixed DNA substrates (see 'Materials and Methods' section). (**B**) General principle of the roadblock assay. Enzymes (circles) are coloured according to their site. Enzymes bound to the site are shown as solid colour; sliding enzymes are shown as transparent colour. See text for further description. (**C**) An amount of 2 nM DNA (HtH, lanes 1–5; TtT, lanes 5–6) was pre-incubated with 100 nM streptavidin for at least 2 min. Then: the DNA in lanes 2 and 7 were incubated for 5 min with both Type III enzymes; the DNA in lanes 3 and 8 were incubated for 30 min with all three enzymes added simultaneously; and, the DNA in lanes 4, 5, 9 and 10 were incubated for 5 min with either with EcoPI or EcoP15I (as indicated), followed by addition of Tn*21* resolvase and the second Type III enzyme (as indicated), and the reaction incubated for a further 30 min. DNA samples were separated by agarose gel electrophoresis and visualized by ethidium bromide fluorescence (the gel image has been inverted to improve visual clarity). The sizes of the marker DNA are indicated in kilo bases (middle lane). DNA fragments of 1500 bp and smaller were not visible after staining and so that part of the gel is not shown.

ATPase rates are low relative to the cleavage rate (5,20,21). Based on the distances between the sites, these rates suggest motor coupling values of many tens of base pairs for each ATP hydrolysed, quite different to typical values for bona fide translocases of one base pair for each ATP [e.g. (22)]. It has been suggested that passively formed 3D DNA loops observed by AFM could allow the motor to shorten the intersite distance between a pair of sites and so account for the observed coupling values (16). However, DNA cleavage studies on catenane substrates (23) and measurements of DNA flexibility by tethered particle tracking (20) were both inconsistent with passive DNA looping. It is also difficult to explain using unidirectional translocation schemes how the cleavage of sites in both HtH and TtT orientation occurs while cleavage of sites in head-to-tail (HtT) orientation does not (6,8).

An alternative model proposes that DNA communication occurs by thermally driven 1D Brownian motion along the polynucleotide track (the DNA Sliding Model) (6,8,20,24). In this model the role of ATP is to catalyse initiation of sliding by causing release from the recognition site. ATP hydrolysis does not need to be coupled to motion following initiation, allowing for a lower ATPase rate. This model explains the site orientation selection discussed above and is consistent with other experimental

observations based on DNA cleavage activity. For example, the presence of a free DNA end (i.e. on a linear DNA molecule) either up or downstream of the Type III recognition site makes cleavage inefficient compared to circular DNA (without DNA ends) or linear DNA with capped ends (e.g. the presence of a bulky protein roadblock such as streptavidin) (6,20,24). We have suggested that during sliding the enzyme can dissociate from the free ends and can access them in either direction as a result of the random bidirectional motion. While the Sliding Model does not require 3D looping, it may still play a role in stabilizing the interaction of two enzymes bound at distant sites (15).

To help refine our understanding of the mechanism of communication, we addressed here the non-specific DNA association lifetime of the communicating enzyme species. The sliding model requires a long-lived communicating state that remains active for cleavage throughout its lifetime on the DNA. A long lifetime is vital because 1D diffusion is a redundant search process, with a square-power dependence between the number of individual random steps and the furthest distance searched (25). In the simplest realization of the Sliding Model, the motile species does not need to re-bind its recognition site following initiation of motion. Therefore we reasoned that we should be able to isolate the sliding species on a stretch of DNA without a recognition site and measure its DNA association lifetime. To achieve this we developed a protein-roadblock assay that allowed isolation of the communicating species from its site and demonstrated that DNA occupancy is long-lived on capped DNA (with a lifetime of >3 min). On DNA with free ends, the association lifetime was too short to be measured. These observations are consistent with dissociation from internal sites being disfavoured while the enzymes can readily thread off free DNA ends. The data does not support a role for 3D DNA looping in selecting the site for initiation of a translocating motor.

Consistent with the original observations of DNA cleavage by the Type III RM enzymes (4,5), another prediction of the sliding model is that two sites in an inverted repeat and at least two bound enzymes are required per DNA for efficient cleavage (6,8,20). Previous studies have used enzyme titrations to explore this requirement. Some of these data were consistent with a view that Type III enzymes cannot turnover following DNA cleavage (10,21,26,27); either the enzymes remain tightly associated with the DNA product (as seen for other RM enzymes) or that they are inactivated following cleavage. Other data suggested that turnover could occur but that site co-methylation, product inhibition or the requirement for multiple enzyme binding events limited the cleavage rate at substoichiometric enzyme concentrations (4,5). We re-examined the dependence of DNA cleavage on the concentration of enzyme under *in vitro* buffer conditions that enhance enzyme activity. The results show quantitatively that the Type III enzymes *can* dissociate from DNA following endonucleases activity and re-bind, such that DNA cleavage can occur at substoichiometric concentrations of enzyme relative to DNA sites. In other words Type III RM enzymes can 'turnover' to some extent, as suggested previously (5). However, the observed cleavage rate showed a sigmoid-shaped dependence on protein concentration characteristic of the expected requirement for at least two enzyme complexes per DNA. There was no evidence from the cleavage kinetics for a cooperative mechanism of DNA binding, further disfavouring this as a reason for the formation of passive 3D loops between pairs of enzymes. At low enzyme concentrations turnover likely becomes limited by the low probability of two enzymes being on the same DNA at the same time and by product inhibition by cleaved DNA (5).

MATERIALS AND METHODS

Proteins

EcoPI, EcoP15I and Tn*21* resolvase were purified as described previously (23). Protein concentrations were determined from the absorption at 280 nm using extinction coefficients derived from the aromatic amino acid composition in the predicted amino acid sequences. EcoPI and EcoP15I concentrations are reported in terms of a Res_2Mod_2 heterotetramer, which reflects the relative subunit levels in our enzyme preparations. (Beyond its necessity for accurate determination of protein concentration, interpretation of the data presented in this article does not rely on the absolute stoichiometry.) All other enzymes were obtained from New England Biolabs (MA, USA) and used as recommended by the manufacturer.

DNA

To make pKA9(-R2), a 223-bp region containing a single Tn*21* resolvase *res* site from pKA9 (24), was removed by digestion with XhoI and SmaI, the DNA re-ligated and clones selected by resistance to cleavage by XhoI. To make pKA16.5, the 2693 bp AccI–AccI fragment of pACYC184 was first cloned into the AccI site of pJT1.1 (6) to make pKA16. A region of pKA16 was amplified by PCR using primers 5′-GACGAAGGCTTGAGCGAGGG-3′ and 5′- CGGGTGATGCTGCCAACTTACTG-3′, and the product ligated.

To prepare DNA for the biochemical assays, *Escherichia coli* TOP10 (Invitrogen) or HB101 (Promega) cells were transformed with pKA9(−R1,+N) (24), pKA9(−R2) or pKA16.5, grown in M9 minimal medium supplemented with 37 MBq/l [³H-methyl] thymidine (PerkinElmer, MA, USA) and the DNA extracted either using a QIAGEN plasmid midi kit (QIAGEN, CA, USA) or by density gradient centrifugation in CsCl–ethidium bromide. pKA9(−R1,+N) was incubated with NdeI (for HtH DNA) or pKA9(−R2) was incubated with PciI (for TtT DNA). End-labelling of the DNA with biotin was carried out using Klenow (3′–5′ exo⁻) polymerase and biotin–dUTP. The labelled DNA was purified by phenol/chloroform extraction followed by ethanol precipitation.

DNA concentrations were determined from absorbance at 260 nm, assuming an extinction co-efficient of 0.02 ml/ μg/cm and a DNA molecular weight of 6.6×10^5 Da/kb.

Molecular weight markers were obtained from Fermentas (Vilnius, Lithuania).

Resolvase order-of-addition roadblock assay

An amount of 2 nM of the linear, biotinylated forms of pKA9(−R1,+N) or pKA9(−R2) were pre-incubated for at least 1 min at 25°C in Buffer R+ [50 mM Tris–HCl, pH 8.0, 50 mM KCl, 10 mM MgCl$_2$, 1 mM DTT and 0.01% (w/v) BSA] supplemented with 4 mM ATP, and, where required, 100 nM streptavidin. Each of the enzymes was diluted and stored on ice: the first Type III enzyme to be added was diluted in Buffer R+; Tn*21* resolvase was diluted in Buffer TD$^+$ [0.1 mM Tris–HCl, pH 8.0, 7.5 mM K glutamate, 1 mM EDTA, 0.01% (w/v) BSA, 4 mM ATP]; and the second Type III enzyme to be added was diluted in Buffer R+ supplemented with either 4 mM ATP, or 4 mM ATP and 2.2 µM streptavidin. All reactions were mixed by hand using a vortex mixer, giving an error in the reaction times of ±0.5 s. To start the reaction, the first Type III enzyme was added as a 20-fold dilution, to the concentrations indicated. After the first incubation period (t_1), a 0.05 volume of resolvase was added to give a final concentration of 200 nM. After the next incubation period (t_2), a 0.048 volume of the second Type III enzyme was added to a final concentration of 15 nM. To get $t_1 = 0$, the aliquots containing the first Type III enzyme and the Tn*21* resolvase were pipetted onto the side of the reaction tube above the DNA solution. The reaction was initiated by touching the reaction tube onto the vortex mixer so that all three volumes mixed at the same time (with the above error). To get $t_1 = 0$ and $t_2 = 0$, the same procedure was carried out except all three proteins were pipetted onto the side of the tube above the DNA solution. To get $t_2 = 0$, the Tn*21* resolvase and the second Type III enzyme were aliquoted into a fresh tube and the pre-incubation reaction was added directly at the end of the t_1 period.

Following addition of all three enzymes, the reaction was allowed to continue for 30 min (t_3) and then stopped by addition of a 0.5 volume of STEB buffer [0.1 M Tris–HCl, pH 7.5, 0.2 M EDTA, 40% (w/v) sucrose, 0.4 mg/ml bromophenol blue]. A 0.1 volume of biotin [0.2 mg/ml in 50 mM Tris–HCl (pH 8.0)] was added to each aliquot and the samples heated for 5 min at 80°C to prevent anomalous electrophoretic mobility due to bound streptavidin. The samples were heated for a further 20 min at 67°C and chilled on ice. The substrates and products were separated by agarose gel electrophoresis and the DNA bands quantified by scintillation counting.

DNA cleavage reactions

pKA16.5 (2 nM) was pre-incubated for at least 1 min at 25°C in Buffer R [50 mM Tris–HCl, pH 8.0, 50 mM KCl, 10 mM MgCl$_2$, 1 mM DTT] supplemented with 4 mM ATP, and 0.01% (w/v) BSA where indicated. Reactions were initiated by adding the Type III RM enzyme at the concentrations indicated, incubated at 25°C for the times indicated, and quenched by addition of a 0.5 volume of STEB buffer. The DNA substrates and products were

separated by agarose gel electrophoresis and the DNA bands quantified by scintillation counting.

RESULTS AND DISCUSSION

A roadblock assay to measure the lifetime of the communicating Type III enzymes

The communication between two distant Type III recognition sites can be interrupted by the binding of a bulky protein roadblock at a specific DNA location intervening the sites, for example Lac repressor to its operator (5) or the site-specific recombinase Tn*21* resolvase to *res* (6). The underlying principle of our assay was to allow communication to initiate from a single Type III recognition site and to subsequently add a protein roadblock to divide the DNA into two domains; one with the recognition site and one without the recognition site. In the sliding model, communication is bidirectional and thus, upon addition of the roadblock, enzymes will be trapped in both domains. The lifetime of those enzymes in the DNA domain without a site could then be measured to gain insight into the stability of the complex without interference from further enzymes initiating motion in that domain.

To implement the assay, we used mixed linear DNA substrates with one recognition site for EcoPI and one recognition site for EcoP15I (Figure 1A). EcoPI and EcoP15I have very similar amino acid sequences (>90% identity in the Res subunit and >60% identity in the Mod subunit, (3)] and together they can efficiently cleave a mixed substrate (28). By using linear DNA rather than circular DNA we can also test: (i) the effect of the site orientation on the direction of travel and (ii) the effect of capped or free DNA ends on the lifetime of the species.

Cartoon examples of the assays on capped DNA are illustrated in Figure 1B. In the first step, only one of the two enzymes is added (the 'first enzyme'), either EcoPI (*upper DNA*) or EcoP15I (*lower DNA*). These initiate from their specific sites and start to move along the entire non-specific DNA. In step two, the partner Type III enzyme (the 'second enzyme') and the roadblock are added. The roadblock is three Tn*21* resolvase dimers bound to a single *res* site. DNA-binding by Tn*21* resolvase is rapid under the conditions used here—the second order DNA-binding rate has been estimated as ~1 × 10^9/M/s and binding of the *res* site by three resolvase dimers would be complete within 50 ms (29). Recombination reactions do not occur as there is only one *res* site. The second Type III enzyme cannot move past the roadblock, even when added simultaneously with Tn*21* resolvase (see below). Therefore, cleavage at the site of the first enzyme cannot occur. However, some of the first enzyme molecules will be in the domain containing the site for the second enzyme and thus cleavage at that site can occur. So, if EcoPI were added first, cleavage would only occur at the EcoP15I site, and *vice versa* (Figure 1B). The readout for the presence of the communicating species on DNA is thus DNA cleavage at the site of the second enzyme following addition of the roadblock.

The assay was first tested by following the efficiency of DNA cleavage at a reaction endpoint using equal concentrations of EcoPI and EcoP15I (15 nM of each), and capped linear DNA (2 nM) with two sites in either HtH repeat (lanes 1–5, Figure 1C) or TtT repeat (lanes 6–10). In the absence of resolvase, both enzymes could communicate and cut the DNA with >99% efficiency. Cleavage was distributed ∼50:50 between the two sites (lanes 2 and 7) as expected, since both sites have local sequences which are identical (9). When both Type III enzymes and Tn21 resolvase were added simultaneously, DNA cleavage was instantaneously blocked (lanes 3 and 8). DNA binding and/or initiation of communication by the Type III enzymes therefore must be substantially slower than the binding of the Tn21 resolvase dimers. In contrast, when one of the Type III enzymes was incubated for 5 min with the DNA prior to addition of the roadblock and the second Type III enzyme, DNA cleavage could occur but was asymmetrically distributed (lanes 4, 5, 9 and 10); when EcoPI was added first, cleavage occurred at the EcoP15I site while when EcoP15I were added first, cleavage occurred at the EcoPI site. The same results were obtained regardless of the relative orientation of the Type III sites.

It is difficult to explain these results based on models in which DNA communication is by unidirectional translocation. The data show that enzymes can move both downstream of their site (i.e. as measured using the HtH DNA) and upstream of their site (i.e. as measured using the TtT DNA). A translocation model involving bidirectional motion should allow cleavage of HtT DNA, but this is not seen. This data is also difficult to reconcile with models where passive 3D looping is used to select a distant site to initiate translocation. If the observed cleavage were due to the first enzyme maintaining a DNA loop over the roadblock, the second enzyme should also be able to perform the same feat, allowing cleavage at both sites. Instead the data are most consistent with the bidirectional motion of the Sliding Model. In this case the enzyme maintains its orientation set by the original binding event but moves either 'forwards' or 'in reverse' in a random manner. The relatively inefficient cleavage can be explained in terms of the numbers and distribution of sliding species along the DNA and on the relative size of the DNA domain containing the second enzyme site; these points are considered in more detail below and in Figure 2 and the Supplementary Data.

Establishing a pre-incubation time for the roadblock assay

To use this assay to study the communicating species in more detail, we used the HtH substrate and modulated the following variables (Figure 2A):

(i) The incubation times between adding the different protein components

The pre-incubation time allowed for the first Type III enzyme to initiate communication was called t_1 (Figure 2A). During this period, the endonuclease starts to move up and downstream of its site, eventually exploring the full length of the DNA or dissociating.
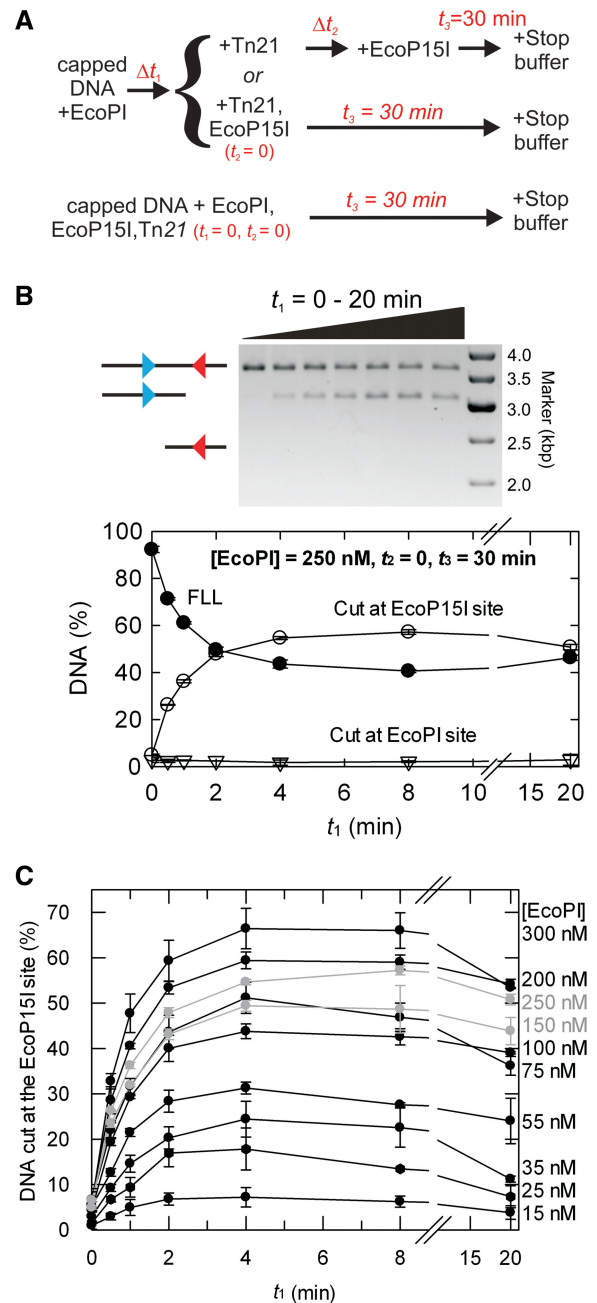

Figure 2. Time- and enzyme-dependent changes in the roadblock assay and the relationship between t_1 and the concentration of EcoPI. (**A**) Definitions of the times used in the roadblock assay with capped DNA. (**B**) Extent of DNA cleavage as a function of different t_1 times at 250 nM EcoPI. FLL is the substrate DNA (Figure 1A). The ethidium bromide-stained gel image has been inverted for clarity. See legend to Figure 1 for comments on size resolution on agarose gels. (**C**) Extent of DNA cleavage at the EcoP15I site (other data not shown) as a function of different t_1 times and concentrations of EcoPI (as indicated). Quantified data is the average of at least two repeat experiments, with the errors bars showing the SD. The relationship between the cleavage at $t_1 = 4$ min and the EcoPI concentrations is shown in Supplementary Figure S1A. The background cleavage at the EcoPI and EcoP15I sites is quantified in Supplementary Figure S4A. The data in grey (150 and 250 nM EcoPI) were carried out with an EcoPI preparation with different specific activity to the other reactions.

The time between addition of the Tn*21* resolvase road-block and the addition of the second Type III enzyme was called t_2. During this period, a Type III enzyme that is trapped in the DNA domain without its recognition site can continue to slide or dissociate from the DNA. Dissociated enzymes will not be replenished because the roadblock prevents communication with the domain containing the recognition site. Following addition of the second Type III enzyme, the third incubation period was called t_3. This was a fixed time during which any of the first enzymes that were still bound to the DNA could communicate with the second Type III enzyme and cut the DNA. The amount of DNA cleavage would give a measure of DNA occupancy by the first Type III enzyme. As $t_1 \to \infty$, we expected the system to approach an equilibrium distribution of bound enzymes such that the cleavage readout would reach a maximum value. As $t_2 \to \infty$, we expected all of the first enzymes to dissociate such that the cleavage readout would tend towards zero. The t_3 incubation time was fixed at 30 min, conditions that were sufficient to give reaction endpoints (data not shown) and which, for technical reasons, gave an ample time-window for the processing of multiple reaction samples in parallel.

(ii) The relative concentrations of the Type III enzymes

The concentration of the first Type III enzyme added was also varied to measure the effect on the rate and extent of loading (during t_1) and on the rate of dissociation (during t_2). In all of the subsequent assays we used EcoPI as the first Type III enzyme added, with its concentration varied between 15 and 300 nM relative to 15 nM EcoP15I. We were unable to carry out the equivalent experiments using EcoP15I as the first enzyme because concentrations of this enzyme >15 nM caused inhibition of cleavage under these conditions [(24), unpublished data].

We anticipated that the approach to the steady-state during t_1 would be a multi-step process involving specific site binding, initiation due to ATP hydrolysis, bidirectional diffusion and dissociation (see discussion below and the Supplementary Data). Notwithstanding this complexity, we needed to measure this step to ensure saturation of the DNA to help in the measurement of the lifetime during t_2. We examined the effect of varying t_1 on capped HtH DNA at various EcoPI concentrations and with $t_2 = 0$ to maximize the number of EcoPI enzymes that could cut the DNA upon addition of Tn*21* resolvase (i.e. dissociation would be minimized). To obtain $t_2 = 0$, Tn*21* and the second Type III enzyme were added simultaneously to the DNA. To obtain $t_1 = 0$ and $t_2 = 0$, Tn*21* and both Type III enzymes were added simultaneously to the DNA.

An example gel and the corresponding quantified data from repeat experiments are shown in Figure 2B for reactions using 250 nM EcoPI. As t_1 was increased from 0 to 20 min, the amount of cleavage at the EcoP15I site increased to a maximum of ~57% at 8 min. At 20 min, the amount of cleavage at the EcoP15I site decreased slightly. This reduction on extended incubation with EcoPI suggests that: (i) EcoPI becomes inactivated as a function of time, decreasing the available enzyme pool;

and/or (ii) that co-methylation of the EcoPI site (5), due to contaminating *S*-adenosyl methionine in the EcoPI protein preparations (9), reduces the number of sites available to initiate sliding as a function of time. Very little cleavage at the EcoPI site was observed regardless of pre-incubation time, consistent with the idea that Tn*21* is an efficient roadblock at these concentrations of Type III enzyme (see below). This also illustrates an important feature of Type III activity—that cleavage of DNA with a single recognition site is very inefficient unless a second enzyme can communicate following initiation at a distant location (10).

The above experiment was then repeated at a range of EcoPI concentrations. The dependence on t_1 of cleavage at the EcoP15I site is shown in Figure 2C for 15–300 nM EcoPI. The data were obtained using different Type III enzyme preparations and hence we observed some variation in relative specific activity; batch-to-batch variation has also been observed in DNA-binding assays (our unpublished data). In all cases there is an increase in cleavage up to ~4 min followed by a decrease. The dependence of the cleavage at the EcoP15I site at $t_1 = 4$ min as a function of EcoPI concentration is shown in Supplementary Figure S1.

As shown previously (24), an increase in enzyme concentration leads to an increase in the number of Type III enzymes on the DNA and a corresponding increase in cleavage (Figure 2C and Supplementary Figure S1). Since the signal saturates <100%, there must be some dissociation of these enzymes (otherwise at the highest concentration, 300 nM EcoPI, we would expect approximately 150 EcoPI enzymes per DNA which would give >99% cleavage at the EcoP15I site). The temporal relationship between the percentage of cleavage at the EcoP15I site and the number of EcoPI enzymes on the DNA is complex (discussed below), but we estimate that at saturating EcoPI concentrations, between two and five EcoPI molecules are associated with non-specific DNA (Supplementary Data). We suggest that the relatively slow approach to the steady state (Figure 2C) is most likely due to the coupling of a slow ATPase rate to the release from the site. The maximum number of enzymes that can be loaded on the DNA is therefore limited by: enzymes waiting at the recognition site to initiate following slow ATP hydrolysis; and a finite sliding lifetime that result in dissociation of enzymes from internal DNA sites. The latter point is explored in more detail in the next experiments. Although, we cannot rule out that the communication event is also a rate-limiting process, data below suggests this is not the case.

Previously we have used Monte Carlo (MC) approaches to simulate the sliding process to examine spatial distributions of enzymes at reaction endpoints (6,24). These simulations did not try to recapitulate the reaction in real time. To use similar approaches to simulate the roadblock assay for comparison with the reaction profiles in Figure 2, we would need to have accurate measures of several rate constants; DNA binding and dissociation, release from the site, sliding and dissociation during sliding. Unfortunately, MC simulations of sliding reactions are slow, even when parallelized on a fast PC, as a large

number of individual sliding steps can occur between other steps such as binding or dissociation, etc. This means that a single simulation can take tens of hours. Since many of the kinetic parameters are not known, the parameter space would need to be iteratively explored to find conditions which matched the empirical data. This was not realistic given the slow simulation time.

The effectiveness of resolvase as a roadblock in this assay can be assessed by measuring the amount of cleavage at the EcoPI and EcoP15I sites when $t_1 = 0$ and $t_2 = 0$, conditions where all three enzymes are mixed with the DNA at the same time. The background cleavage at the EcoPI is only 2% and is not affected by the change in EcoPI concentration (Supplementary Figure S4A). The background cleavage at the EcoP15I site shows dependence upon EcoPI concentration and reaches a maximum of ~6% (Supplementary Figure S4A). Therefore, at elevated EcoPI concentrations there is a small chance of bypassing the *res* site, either before resolvase binds or during transient resolvase dissociation events. Nonetheless, this represents an acceptably low background value.

The DNA association lifetime of EcoPI on capped DNA

To determine the stability of the sliding species isolated away from its recognition site, we measured the effect of varying t_2 on the cleavage at the EcoP15I site following a fixed pre-incubation time (t_1) of 4 min. Compared to the complex series of steps during the approach to equilibrium during t_1 (above), we anticipated that any dissociation process would be more tractable. For situations where a single EcoPI enzyme is bound in the EcoP15I domain, the dissociation kinetics would be defined by a single unimolecular rate process (Supplementary Figure S3). Given our estimates of the number of EcoPI molecules on a DNA, any deviation from this relationship would be smaller than the data scatter and would still allow reasonable estimation of the stability of the interaction with non-specific sites (see below, and the Supplementary Data).

An example gel and the corresponding quantified data from repeat experiments are shown in Figure 3A for reactions using 250 nM EcoPI. Over 16 min, the amount of cleavage at the EcoP15I site dropped from ~52% to a background level of ~7% while the cleavage at the EcoPI site remained at a background level of ~2%. This is consistent with slow dissociation of the EcoPI molecules from the EcoP15I domain following addition of resolvase.

The experiment was then repeated at a range of EcoPI concentrations (25–300 nM) and the decrease in EcoP15I cleavage as a function of t_2 was fitted to Equation (1):

$$P = A \cdot \exp\left(-\frac{t_2}{t_S}\right) + offset \tag{1}$$

where, P is the percentage of cleavage at the EcoP15I site, A is the maximum EcoP15I cleavage at $t_2 = 0$ (for $t_1 = 4$ min), *offset* is the percentage background cleavage (Supplementary Figure S4) and t_S is the lifetime of the EcoPI sliding state. Example data and the corresponding fits to Equation (1) are shown in Figure 3B for experiments at 200, 55 and 25 nM EcoPI. The dependences of t_S,
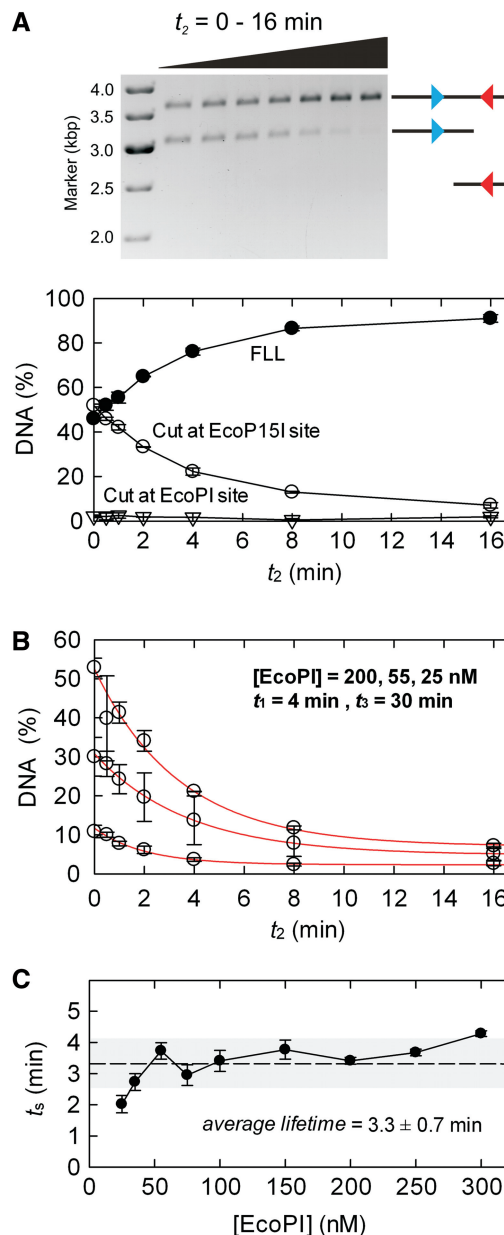

Figure 3. The lifetime of the EcoPI sliding state estimated from the relationship between t_2 and the concentration of EcoPI. (**A**) Extent of DNA cleavage as a function of different t_2 times at 250 nM EcoPI. FLL is the substrate DNA (Figure 1A). The ethidium bromide-stained gel image has been inverted for clarity. See legend to Figure 1 for comments on size resolution on agarose gels. (**B**) Extent of DNA cleavage at the EcoP15I site as a function of different t_2 times for the concentrations of EcoPI indicated. Quantified data is the average of at least two repeat experiments, with the errors bars showing the SD. The red line represents least squares fits to Equation (1). (**C**) The relationship between t_s values returned from least squares fits to Equation (1) and the EcoPI concentration, with the error bars representing the standard error from the fits. The dashed line and grey box are the average and SD, respectively, of the data. The relationships between EcoPI concentrations and the A and *offset* values from least squares fits to Equation (1) are shown in Supplementary Figures S1B and S4B. The background cleavage at the EcoPI and EcoP15I sites is quantified in Supplementary Figure S4B.

A and *offset* on the full range of EcoPI concentrations are shown in Figure 3C, Supplementary Figure S1B and Supplementary Figure S4B, respectively.

As discussed in the Supplementary Data, the use of Equation (1) assumes dissociation of a single EcoPI species. Within the estimated range of 2–5 EcoPI molecules per DNA at maximum saturation, the majority of DNA will still only have a single EcoPI enzyme in the EcoP15I domain. However, the influence of those DNA with multiple EcoPI molecules in that domain will be to cause systematic deviations from Equation (1) that in turn cause an overestimation of the association lifetime (Supplementary Figure S3). As a function of increasing EcoPI concentration, the t_s values did show a slight systematic increase (Figure 3C). However, the experimental scatter in the data is quite significant, making robust interpretations more difficult. The mean t_s value gives an average lifetime for the EcoP15I cleavage state of 3.3 ± 0.7 min. Given the error range and the distribution of the scatter, we suggest that this value is a good estimate of the lifetime of a single EcoPI molecule during communication.

The dissociation of EcoPI enzymes during the t_2 incubation period indicates that the Type III enzymes have a finite lifetime on DNA and can dissociate from internal sites. One of the arguments against sliding as an effective mode of communication is that to travel long distances would require a long association lifetime. Taking into account the range of measured diffusion co-efficient (*D*) for 1D DNA sliding, e.g. (30,31), a 3.3 min lifetime would allow a Type III enzyme to communicate over average distances of 1.85 kb (for $D = 0.001 \,\mu m^2/s$) to 18.5 kb (for $D = 0.1 \,\mu m^2/s$). Given the high frequency of Type III sites in bacteriophage genomes (21,32), these values would be more than sufficient to allow communication between a pair of Type III sites. It is possible that the lifetime might be extended under other circumstances by the enzyme re-binding to recognition sites during sliding.

The relationship between the fitted *A* values and the EcoPI concentration indicates a saturation curve similar to that seen for the previous data (Supplementary Figure S1B), as expected. Small differences between the absolute amplitudes at each concentration most likely reflect differences in specific activity of EcoPI preparations used throughout this study. The low levels of background cleavage at the EcoPI and EcoP15I sites were similar to those seen above (Supplementary Figure S4A and B).

The DNA association lifetime of EcoPI on uncapped DNA

One of our interpretations of previous DNA cleavage data is that during sliding on linear DNA, Type III enzymes have a tendency to dissociate readily from free DNA ends (20). This can be prevented by capping the ends with a reflecting roadblock, for example streptavidin. We predicted that if we used uncapped linear DNA in the roadblock assay, t_s would be significantly reduced. Since the roadblock assay relies on efficient DNA cleavage as readout of DNA-bound EcoPI molecules, it was necessary to use biotin-labelled DNA but to only add streptavidin

when EcoP15I was added (Figure 4A), i.e. the DNA remained uncapped until the t_3 incubation period when efficient DNA cleavage needed to occur. The second-order rate of association of streptavidin with biotin is $\sim 2 \times 10^7$/M/s (33), which would give >96% DNA ends bound in 1 s upon addition of streptavidin. Any EcoPI molecules that were still bound to the EcoP15I domain when streptavidin binds could then be maintained in the DNA bound state, so allowing readout of cleavage at the EcoP15I site. The value for t_1 was kept as 4 min as longer pre-incubation times did not alter the following results (data not shown).

Results are only shown for 300 nM EcoPI and for relatively short t_2 times (Figure 4B). Compared to the capped DNA (Figure 2), very little cleavage of the EcoP15I site above background could be measured at $t_2 = 0$. In other words, even following extensive pre-incubation at an elevated EcoPI concentration, very few sliding enzymes were bound to the DNA. Consequently, the changes in EcoP15I cleavage at $t_2 = 5$ and 30 s relative to $t_2 = 0$ were smaller than the data scatter due to experimental error, making it impossible to extract meaningful kinetic values for t_s on uncapped DNA.

If we assume that each EcoPI enzyme that reaches an uncapped DNA end will spontaneously dissociate (due to loss of important protein–DNA contacts), then the shorter lifetime on uncapped DNA will be determined mainly by the time it takes on average for a Type III enzyme to reach a DNA end. During the pre-incubation period (t_1), EcoPI initiates from its recognition site, which is 1205 and 2443 bp from the free ends (Figure 1A). Using typical diffusion coefficients, and an analytical solution for diffusion-to-capture with two absorbing boundaries (25), we can estimate a mean time to reach a DNA end of between 1.7s (for $D = 0.1 \,\mu m^2/s$) to 170s (for
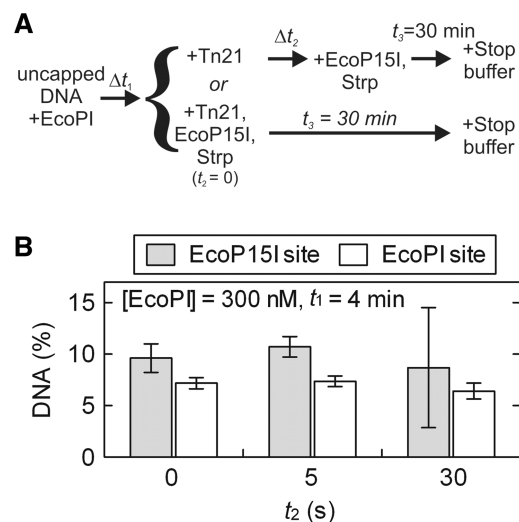

Figure 4. The lifetime of EcoPI DNA sliding on uncapped DNA is too short to be measured in the roadblock assay. (**A**) Definitions of the times used in the roadblock assay with uncapped DNA. (**B**) The extent of cleavage at either the EcoP15I or EcoPI sites on HtH uncapped DNA using 300 nM EcoPI is shown for $t_2 = 0$, 5 or 30 s. The data is the average of at least two repeat experiments, with the errors bars showing the SD.

$D = 0.001 \, \mu m^2/s$). With the slower diffusion co-efficient, one would expect to observe reasonable levels of EcoP15I cleavage at $t_2 = 0$ as a 170 s lifetime is on a similar order to the observed lifetime at internal sites (of 198 s, Figure 3C). At the faster rate, the enzymes are likely to have left the DNA before initiation of a second sliding event and so, at best, only a single enzyme would be found on the DNA. If an EcoPI enzyme were in the EcoP15I domain when the Tn21 resolvase were added, then it would become trapped in a 1176-bp region of DNA with one free DNA end and one reflecting boundary (the resolvase proteins). Assuming a uniform distribution of sliding enzymes along the DNA domain, the average distance between an EcoPI molecule and the free DNA end would be ~588 bp. Using a diffusion-to-capture model with one reflecting boundary and one absorbing boundary (25), we can estimate a mean time to reach the free DNA end of between 200 ms (for $D = 0.1 \, \mu m^2/s$) and 20 s (for $D = 0.001 \, \mu m^2/s$). Given the time taken by streptavidin to bind (see above), at the faster diffusion co-efficient the EcoPI molecules may have exited the DNA before the end becomes capped. Conversely for the slower rate we would have expected to be able to capture some sliding molecules.

Our interpretation of the data on the uncapped DNA is that we cannot measure the lifetime of EcoPI on uncapped DNA as the number of enzymes on the DNA is too low to capture significant amounts of EcoPI in the EcoP15I domain; i.e. at equilibrium, the majority of the DNA molecules do not have any enzymes in the act of sliding (note, however, that the recognition sites may be saturated with enzymes yet to initiate). Given that we can capture sliding enzymes on capped DNA with a lifetime of ~198 s, this suggests that Type III enzymes must move with a 1D diffusion co-efficient $>> 0.001 \, \mu m^2/s$. This in turn suggests that the slow kinetics observed in Figure 2 are due to steps other than sliding.

Evidence for turnover of Type III restriction enzymes following DNA cleavage

Previous analysis of DNA cleavage profiles have suggested that a minimal requirement for Type III endonuclease activity is the presence of two enzyme complexes on one DNA, one to cut the 'top' strand of the dsDNA, one to cut the 'bottom strand' (5,9,34). The sliding model proposes that one of these enzymes is bound to a recognition site and that the second enzyme initiated sliding elsewhere and has then collided with the static enzyme in a 'head-on' orientation (8). This brings the endonuclease domains into contact at the correct cleavage location on the DNA, 25- to 27-bp downstream of the site. Following cleavage however, an uncertainty remains as to whether Type III RM enzymes can turnover following cleavage (5), or not (9,21,27,35).

We re-tested the relationship between the efficiency of DNA cleavage and Type III enzyme concentration by measuring the cleavage profiles at a fixed time point of 2 h using a plasmid substrate with pairs of EcoPI and EcoP15I sites in inverted repeat (Figure 5A). We used two buffer conditions, one with 100 μg/ml Bovine Serum

Albumin (BSA) and one without BSA (see 'Materials and Methods' section) and either EcoP15I alone (Figure 5B) or EcoPI alone (data not shown). The efficiency of DNA cleavage was measured from the amount of covalently closed circular (CCC) DNA remaining after 2 h. Quantified data from repeat experiments with or without BSA and with either EcoP15I or EcoPI are shown in Figure 5C.

In the absence of BSA, both enzymes required a molar excess of enzyme compared to DNA sites to produce efficient cleavage (nominally defined as ≤10% CCC remaining after 2 h) (Figure 5C). In the presence of BSA, an increase in efficiency was observed. At substoichiometric concentrations of enzyme to DNA site, the dependence of cleavage efficiency on enzyme concentration varied according to the enzyme and buffer conditions. For EcoPI in BSA, efficiency reduced as the enzyme concentration reduced, until little or no cleavage was observed at an enzyme-to-site ratio of ~1:4. For EcoP15I in BSA, the overall cleavage efficiency was elevated compared to EcoPI, and partial DNA cleavage was still observed at an enzyme-to-site ratio of ~1:10.

The DNA cleavage data with BSA buffers from Figure 5C was reanalysed to compare the fraction of CCC DNA remaining after 2 h against the enzyme-to-site ratio (Figure 5D). The error bars in the CCC values come directly from the experimental data in Figure 5C. The error bars in the enzyme:sites ratios were estimated based on experimental uncertainty in the determination of protein and DNA concentrations of ±10%, as considered by us previously in refs (22,36) (discussed below). Also shown in Figure 5D are three theoretical lines for different cleavage models: (i) independent binding with no turnover (blue line), where each enzyme binds its site independently and cannot turnover following DNA cleavage (the enzymes are inactivated or product release is terminally slow); (ii) cooperative binding with no turnover (green line), where the binding of two sites on the same DNA by two enzyme complexes is cooperative (for example due to 3D DNA looping) and following DNA cleavage the enzymes cannot turnover; and, (iii) independent or cooperative binding schemes where the enzymes can rapidly turnover (*red line*), and cleavage is complete within 2 h independent of protein concentration. Under conditions of rapid turnover it is not necessarily possible to distinguish between the independent and cooperative modes of binding from the endpoints at 2 h alone.

The cleavage data for EcoPI and EcoP15I both show some evidence for turnover during DNA cleavage (Figure 5D), with the effect being most convincing for EcoP15I. It is unlikely that this is wholly due to inaccuracies in the protein or DNA concentrations. The largest error in determining DNA and protein concentrations is in calculation of theoretical extinction coefficients (22,36). Typical error ranges for both are ±5% (SD), with maximum errors in the range ±10%. The x-axis error bars in Figure 5D show a range according to these maximum limits. Given these errors, our results are still consistent with some degree of turnover. To explain away our conclusions would require errors
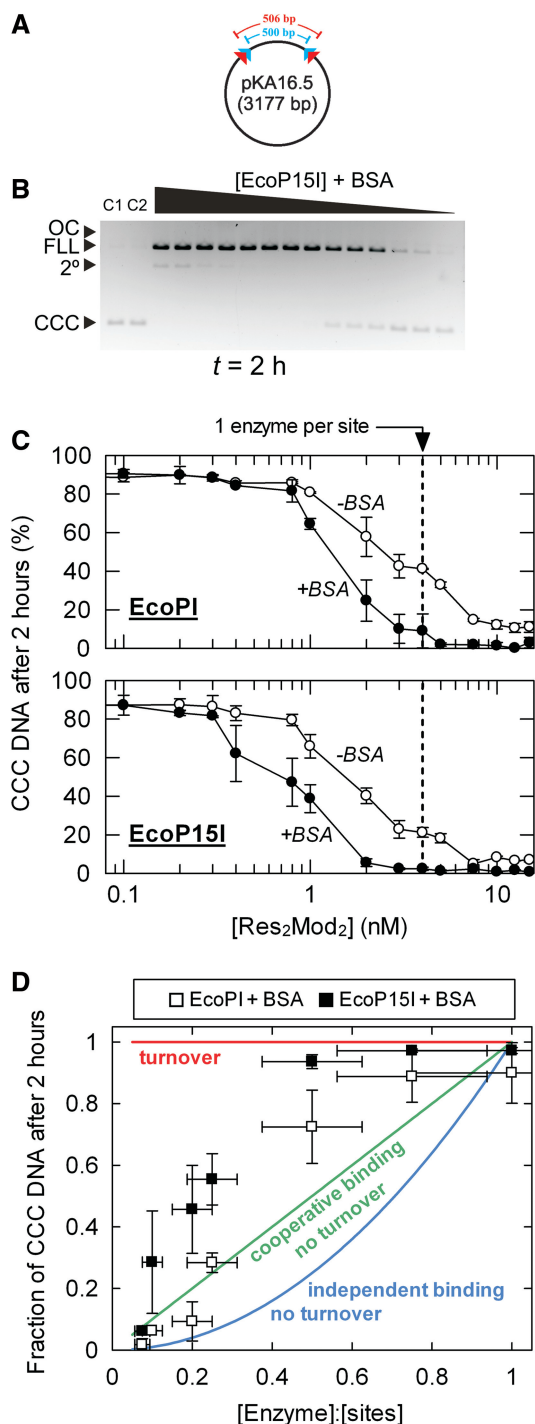
Figure 5. Bovine Serum Albumin increases the efficiency of *in vitro* plasmid DNA cleavage and reveals evidence of partial turnover in the endonuclease reaction. (**A**) Plasmid DNA substrate, with the spacing between the HtH DNA arcs shown for EcoPI (blue) and EcoP15I (red). NB on plasmid DNA, cleavage can occur by communication across either HtH or TtT DNA arcs. (**B**) Example ethidium bromide-stained agarose gel showing separation of the DNA control, substrate and cleavage products with different concentrations of EcoP15I (0–15 nM) following 2 h incubation in the presence of BSA. See legend to Figure 1 for comments on size resolution on agarose gels. C1 is DNA loaded directly onto the gel; C2 is DNA loaded following 2 h incubation in reaction buffer. The mobility of CCC, nicked (Open Circular, OC) and FLL are indicated. Also indicated is a ~2.7 kb band that results from cleavage at the second Type III site (2°), at elevated EcoP15I concentrations. All four bands were used to quantify the extent of DNA cleavage. (**C**) Cleavage of CCC DNA after 2 h at different concentrations of EcoPI or EcoP15I in the absence (white circles) or presence (black circles) of BSA. The data is the average of at least two repeat experiments, with the errors bars showing the SD. (**D**) Correlation between the fractional cleavage of the CCC DNA and the ratio of enzyme to recognition site. For details of error bars and the simulated lines, see main text.

of ±40–50%, much larger than would be normally expected. Nevertheless, turnover was quite inefficient and below a threshold (e.g. 0.2 nM EcoP15I), no cleavage above background was observed after 2 h. Similar qualitative observations were made by Meisel *et al.* (5) using EcoP15I on multi-site DNA. This low efficiency of turnover can be explained on the basis of kinetic constraints, which are discussed below.

BSA clearly increased the cleavage efficiency of both enzymes (Figure 5C), most likely by preventing a decrease in specific activity during incubation in reaction buffer. Our original analysis of the cleavage stoichiometry of EcoPI was carried out in buffers without BSA (9). Under those conditions we found that DNA cleavage required an enzyme:site ratio >1, which was consistent with the Type III enzymes being inefficient at turnover following DNA cleavage. More recently we started using BSA in our Type III reaction buffers (20), as we noted that this improved enzyme activity. As similar improvements could be made using Eppendorf Lobind tubes or by addition of 0.0025% (v/v) Triton X-100 (data not shown), the most likely effect of BSA is to block binding of EcoPI and EcoP15I to the plastic of the reaction tubes. Recent data on the Type I RM enzymes has also demonstrated that turnover following DNA cleavage can occur if specific *in vitro* reaction conditions are provided, overturning similar long-held views (36,37). The relevance of turnover for a restriction enzyme *in vivo* is discussed in these reports.

DNA cleavage rates are consistent with the independent binding of at least two Type III enzymes at two DNA sites

The data in Figure 5 shows evidence for partial enzyme turnover but cannot distinguish between independent and cooperative models for DNA binding. To help provide evidence for one or other model we measured the DNA cleavage rate at different concentrations of EcoP15I. In the sliding model, cleavage can only occur when two enzymes bind the same DNA at the same time. As the enzyme concentration is lowered, the probability of two enzymes being on the same DNA at the same time will drop, eventually limiting the cleavage rate. For cooperative binding, we would expect to see a rapid burst in the cleavage that corresponds to the concentration of enzyme. For example, if we added 2 nM EcoP15I to 2 nM DNA (4 nM sites), 1 nM of the DNA would be loaded cooperatively with pairs of enzymes required for cleavage. Thus there would be a rapid phase of cleavage with 50% amplitude corresponding to this loading. For an independent binding scheme at the same concentrations, the maximum amplitude of the burst phase would be 25% (corresponding to a binomial distribution—viz. Figure 5D). This burst

could be even lower if cleavage requires multiple loading and initiation events.

An example gel and the corresponding quantified data from repeat experiments are shown in Figure 6A for 2 nM EcoP15I. The DNA cleavage rate can be fitted to a single exponential relationship (either from the drop in CCC DNA or the increase in full length linear, FLL, DNA). There was no clear evidence for a burst phase during the reaction. The concentration of nicked DNA (OC—open circle) remained static during the reaction, indicating that the FLL DNA arises from two successive rapid cleavage steps, i.e. the microscopic cleavage rates are not rate-limiting. We repeated these cleavage reactions for a range of EcoP15I concentrations (2–15 nM). Example data for 4, 5 and 7.5 nM EcoPI are shown in Figure 6B. The rate of cleavage increased as the enzyme concentration increased, following a single exponential decay in each case. No clear evidence for burst kinetics was observed at any enzyme concentration (data not shown). Furthermore, the open circle DNA remained level under all conditions. This suggests that the changes in the macroscopic cleavage rate correspond to changes processes before or after the microscopic cleavage steps.

The macroscopic cleavage rates determined from the single exponential fits have an approximately sigmoidal relationship with the enzyme concentration (Figure 6C). At a stoichiometric concentration of enzyme and DNA sites (vertical dotted line), the cleavage rate is subsaturated. To attain the maximum cleavage rate requires a >2-fold molar excess of enzymes to DNA sites. Even with generous estimates of the uncertainty in protein and DNA concentrations (i.e. Figure 5D), this still requires an excess concentration of enzyme over sites to achieve the maximum cleavage rate. The data is consistent with a model where efficient cleavage requires the interaction of at least two enzyme complexes per DNA. As the concentration is lowered, the chance of two enzymes being initially loaded onto the same DNA becomes rarer. The cleavage rate therefore becomes limited by the time it takes for an enzyme to dissociate from a DNA molecule and resample the DNA population. In addition, DNA cleavage does not destroy the Type III recognition site. Consequently, binding of the decreasing pool of substrate DNA will be inhibited by the sequestration of binding/initiation/sliding events on the increasing pool of product DNA (5). Unproductive binding events could explain the rapid drop in the cleavage efficiency observed at lowest enzyme concentrations in Figure 5C. We do not necessarily need to invoke a slow dissociation following cleavage to explain our results.

For a linear HtH DNA, the cleavage adjacent to one or other recognition site separates the sites onto separate DNA molecules, so any rebinding cannot lead to communication and cleavage of the remaining intact site. However, for linear TtT DNA or for circular DNA with sites in inverted repeat, the first cleavage event releases a TtT product which still has two sites connected in 1D. What prevents this DNA being further cut? We suggest two possibilities, which are not mutually exclusive; first, the cleaved site is immediately adjacent to a DNA end,
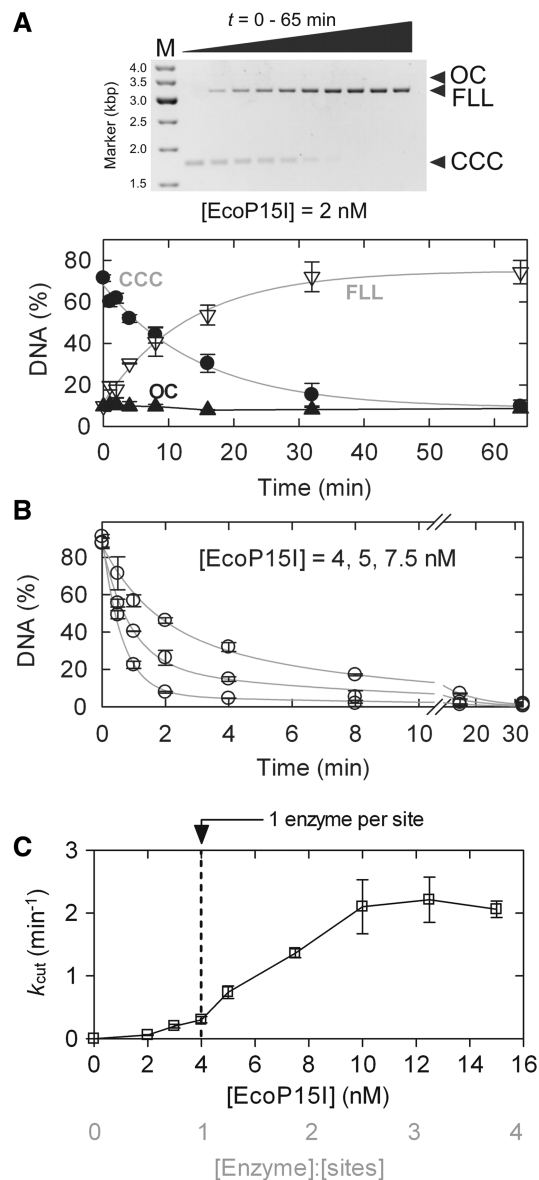

Figure 6. The dependence of the plasmid DNA cleavage rate on the concentration of EcoP15I is consistent with the requirement for multiple enzyme binding events for cleavage. (**A**) Representative ethidium bromide-stained agarose gel (inverted image shown for clarity) and quantified data for the rate of cleavage of 2 nM pKA16.5 using 2 nM EcoP15I. The data is the average of at least two repeat experiments, with the errors bars showing the SD. Lines are least squares fits to single exponential decrease (CCC) or increase (FLL). Both return similar rate constants (not shown). (**B**) The rate of CCC cleavage at (from left to right) 4, 5 and 7.5 nM EcoP15I, with least squares fits to single exponentials (lines). The data is the average of at least two repeat experiments, with the errors bars showing the SD. (**C**) Relationship between the cleavage rate (k_{cut}), determined from least squares fits of the CCC data to a single exponential, and the EcoP15I concentration (the equivalent enzyme:site ratio is also indicated). Errors bars are the standard errors of the fits. The points are joined by straight lines to guide the eye.

and this may affect binding to the site; secondly, the products are DNA with an uncapped end or ends. For a TtT substrate with a site close to an end, this will make communication and thus cleavage very inefficient (24).

CONCLUSIONS

On the basis of the data presented in this article, we make a number of conclusions:

(i) the Type III enzymes can move both up and downstream of their site, consistent with a bidirectional mode of motion;

(ii) initiation produces a stable long-range communication state which dissociates slowly from internal non-specific sites;

(iii) the lifetime on DNA with free ends was shorter than could be measured in our assay. This suggests that the Type III enzymes must rapidly interact with the DNA ends during communication and that these structures allow faster dissociation than internal DNA sites. The data is also consistent with rapid sliding, occurring with a 1D diffusion co-efficient $\gg 0.001\,\mu m^2/s$;

(iv) re-binding to the recognition site during motion is not a necessity as the motile state can be trapped in a DNA segment lacking a recognition site. minutes after release from its site, the isolated form of the enzyme can still participate in DNA cleavage upon collision with a second Type III enzyme. However, we cannot rule out that sliding enzymes can re-associate with recognition sites;

(v) the kinetics of DNA cleavage are consistent with independent binding of endonucleases at each site. Turnover following DNA cleavage can occur but the observed cleavage is limited in efficiency and rate by a requirement for at least two enzymes to be bound per DNA to achieve cleavage, and by product inhibition.

The above observations can be brought together most easily in the context of the previously suggested DNA Sliding Model (8). In contrast, it is difficult to explain the bidirectional motion (Figure 1), slow approach to equilibrium (Figure 2) and long-lived cleavage-competent state (Figure 3) in the context of models that require unidirectional motion (i.e. translocation). An important discrepancy that remains to be resolved is that the AFM data suggests that DNA looped species are long-lived (16–18). We cannot explicitly rule out looping schemes using the experiments here. Further assays need to be developed to corroborate (or definitively refute) a role for DNA looping in the mechanism of Type III enzymes.

SUPPLEMENTARY DATA

Supplementary Data are available at NAR Online: Supplementary Figures 1–4, Supplementary Results and Discussion.

ACKOWLEDGEMENTS

FUNDING

REFERENCES

1. Dryden,D.T., Murray,N.E. and Rao,D.N. (2001) Nucleoside triphosphate-dependent restriction enzymes. *Nucleic Acids Res.*, **29**, 3728–3741.
2. Raghavendra,N.K., Bheemanaik,S. and Rao,D.N. (2012) Mechanistic insights into type III restriction enzymes. *Frontiers Biosci.*, **17**, 1094–1107.
3. Roberts,R.J., Vincze,T., Posfai,J. and Macelis,D. (2010) REBASE–a database for DNA restriction and modification: enzymes, genes and genomes. *Nucleic Acids Res.*, **38**, D234–D236.
4. Meisel,A., Bickle,T.A., Kruger,D.H. and Schroeder,C. (1992) Type III restriction enzymes need two inversely oriented recognition sites for DNA cleavage. *Nature*, **355**, 467–469.
5. Meisel,A., Mackeldanz,P., Bickle,T.A., Kruger,D.H. and Schroeder,C. (1995) Type III restriction endonucleases translocate DNA in a reaction driven by recognition site-specific ATP hydrolysis. *EMBO J.*, **14**, 2958–2966.
6. van Aelst,K., Toth,J., Ramanathan,S.P., Schwarz,F.W., Seidel,R. and Szczelkun,M.D. (2010) Type III restriction enzymes cleave DNA by long-range interaction between sites in both head-to-head and tail-to-tail inverted repeat. *Proc. Natl Acad. Sci. USA*, **107**, 9123–9128.
7. Mucke,M., Reich,S., Moncke-Buchner,E., Reuter,M. and Kruger,D.H. (2001) DNA cleavage by type II restriction-modification enzyme EcoP15I is independent of spacer distance between two head to head oriented recognition sites. *J. Mol. Biol.*, **312**, 687–698.
8. Szczelkun,M.D., Friedhoff,P. and Seidel,R. (2010) Maintaining a sense of direction during long-range communication on DNA. *Biochem. Soc. Trans.*, **38**, 404–409.
9. Peakman,L.J., Antognozzi,M., Bickle,T.A., Janscak,P. and Szczelkun,M.D. (2003) S-Adenosyl methionine prevents promiscuous DNA cleavage by the EcoP1I type III restriction enzyme. *J. Mol. Biol.*, **333**, 321–335.
10. Peakman,L.J. and Szczelkun,M.D. (2009) S-Adenosyl homocysteine and DNA ends stimulate promiscuous nuclease activities in the Type III restriction endonuclease EcoPI. *Nucleic Acids Res.*, **37**, 3934–3945.
11. Singleton,M.R., Dillingham,M.S. and Wigley,D.B. (2007) Structure and mechanism of helicases and nucleic acid translocases. *Annu. Rev. Biochem.*, **76**, 23–50.
12. Stanley,L.K., Seidel,R., van der Scheer,C., Dekker,N.H., Szczelkun,M.D. and Dekker,C. (2006) When a helicase is not a helicase: dsDNA tracking by the motor protein EcoR124l. *EMBO J.*, **25**, 2230–2239.
13. Durr,H., Korner,C., Muller,M., Hickmann,V. and Hopfner,K.P. (2005) X-ray structures of the Sulfolobus solfataricus SWI2/SNF2 ATPase core and its complex with DNA. *Cell*, **121**, 363–373.
14. Szczelkun,M.D. (2011) Translocation, switching and gating: potential roles for ATP in long-range communication on DNA by Type III restriction endonucleases. *Biochem. Soc. Trans.*, **39**, 589–594.
15. Dryden,D.T., Edwardson,J.M. and Henderson,R.M. (2011) DNA translocation by type III restriction enzymes: a comparison of current models of their operation derived from ensemble and single-molecule measurements. *Nucleic Acids Res.*, **39**, 4525–4531.
16. Crampton,N., Roes,S., Dryden,D.T., Rao,D.N., Edwardson,J.M. and Henderson,R.M. (2007) DNA looping and translocation provide an optimal cleavage mechanism for the type III restriction enzymes. *EMBO J.*, **26**, 3815–3825.
17. Crampton,N., Yokokawa,M., Dryden,D.T.F., Edwardson,J., Michael,R., Desirazu,N., Takeyasu,K., Yoshimura,S.H. and

Henderson,R.M. (2007) Fast-scan atomic force microscopy reveals that the type III restriction enzyme EcoP15I is capable of DNA translocation and looping. *Proc. Natl Acad. Sci. USA*, **104**, 12755–12760.

18. Reich,S., Gossl,D., Reuter,M., Rabe,J.P. and Kruger,D.H. (2004) Scanning force microscopy of DNA translocation by the type III restriction enzyme EcoP15I. *J. Mol. Biol.*, **341**, 337–343.

19. Raghavendra,N.K. and Rao,D.N. (2004) Unidirectional translocation from recognition site and a necessary interaction with DNA end for cleavage by Type III restriction enzyme. *Nucleic Acids Res.*, **32**, 5703–5711.

20. Ramanathan,S.P., van Aelst,K., Sears,A., Peakman,L.J., Diffin,F.M., Szczelkun,M.D. and Seidel,R. (2009) Type III restriction enzymes communicate in 1D without looping between their target sites. *Proc. Natl Acad. Sci. USA*, **106**, 1748–1753.

21. Sears,A., Peakman,L.J., Wilson,G.G. and Szczelkun,M.D. (2005) Characterization of the type III restriction endonuclease PstII from Providencia stuartii. *Nucleic Acids Res.*, **33**, 4775–4787.

22. Seidel,R., Bloom,J.G., Dekker,C. and Szczelkun,M.D. (2008) Motor step size and ATP coupling efficiency of the dsDNA translocase EcoR124I. *EMBO J.*, **27**, 1388–1398.

23. Peakman,L.J. and Szczelkun,M.D. (2004) DNA communications by Type III restriction endonucleases - confirmation of 1D translocation over 3D looping. *Nucleic Acids Res.*, **32**, 4166–4174.

24. Schwarz,F.W., van Aelst,K., Toth,J., Seidel,R. and Szczelkun,M.D. (2011) DNA cleavage site selection by Type III restriction enzymes provides evidence for head-on protein collisions following 1D bidirectional motion. *Nucleic Acids Res.*, **39**, 8042–8051.

25. Berg,H.C. (1993) *Random Walks in Biology*. Princeton University Press, Princeton.

26. Moncke-Buchner,E., Rothenberg,M., Reich,S., Wagenfuhr,K., Matsumura,H., Terauchi,R., Kruger,D.H. and Reuter,M. (2009) Functional characterization and modulation of the DNA cleavage efficiency of type III restriction endonuclease EcoP15I in its interaction with two sites in the DNA target. *J. Mol. Biol.*, **387**, 1309–1319.

27. Raghavendra,N.K. and Rao,D.N. (2003) Functional cooperation between exonucleases and endonucleases - basis for the evolution of restriction enzymes. *Nucleic Acids Res.*, **31**, 1888–1896.

28. Kunz,A., Mackeldanz,P., Mucke,M., Meisel,A., Reuter,M., Schroeder,C. and Kruger,D.H. (1998) Mutual activation of two restriction endonucleases: interaction of EcoPI and EcoP15. *Biol. Chem.*, **379**, 617–620.

29. Oram,M., Marko,J.F. and Halford,S.E. (1997) Communications between distant sites on supercoiled DNA from non-exponential kinetics for DNA synapsis by resolvase. *J. Mol. Biol.*, **270**, 396–412.

30. Blainey,P.C., van Oijen,A.M., Banerjee,A., Verdine,G.L. and Xie,X.S. (2006) A base-excision DNA-repair protein finds intrahelical lesion bases by fast sliding in contact with DNA. *Proc. Natl Acad. Sci. USA*, **103**, 5752–5757.

31. Bonnet,I., Biebricher,A., Porte,P.L., Loverdo,C., Benichou,O., Voituriez,R., Escude,C., Wende,W., Pingoud,A. and Desbiolles,P. (2008) Sliding and jumping of single EcoRV restriction enzymes on non-cognate DNA. *Nucleic Acids Res.*, **36**, 4118–4127.

32. Schroeder,C., Jurkschat,H., Meisel,A., Reich,J.G. and Kruger,D. (1986) Unusual occurrence of EcoP1 and EcoP15 recognition sites and counterselection of type II methylation and restriction sequences in bacteriophage T7 DNA. *Gene*, **45**, 77–86.

33. Howarth,M., Chinnapen,D.J., Gerrow,K., Dorrestein,P.C., Grandy,M.R., Kelleher,N.L., El-Husseini,A. and Ting,A.Y. (2006) A monovalent streptavidin with a single femtomolar biotin binding site. *Nat. Methods*, **3**, 267–273.

34. Janscak,P., Sandmeier,U., Szczelkun,M.D. and Bickle,T.A. (2001) Subunit assembly and mode of DNA cleavage of the type III restriction endonucleases EcoP1I and EcoP15I. *J. Mol. Biol.*, **306**, 417–431.

35. Raghavendra,N.K. and Rao,D.N. (2005) Exogenous AdoMet and its analogue sinefungin differentially influence DNA cleavage by R.EcoP15I-Usefulness in SAGE. *Biochem. Biophys. Res. Commun.*, **334**, 803–811.

36. Simons,M. and Szczelkun,M.D. (2011) Recycling of protein subunits during DNA translocation and cleavage by Type I restriction-modification enzymes. *Nucleic Acids Res.*, **39**, 7656–7666.

37. Roberts,G.A., Cooper,L.P., White,J.H., Su,T.J., Zipprich,J.T., Geary,P., Kennedy,C. and Dryden,D.T. (2011) An investigation of the structural requirements for ATP hydrolysis and DNA cleavage by the EcoKI Type I DNA restriction and modification enzyme. *Nucleic Acids Res.*, **39**, 7667–7676.